N90-28642

HIGH TEMPERATURE FATIGUE BEHAVIOR OF HAYNES 188

Gary R. Halford and James F. Saltsman
National Aeronautics and Space Administration
Lewis Research Center
Cleveland, Ohio 44135
and
Sreeramesh Kalluri
Sverdrup Technology, Inc.
NASA-Lewis Research Center
Cleveland, OH 44135

ABSTRACT

The high-temperature, creep-fatigue behavior of Haynes 188 has been investigated as an element in a broader thermomechanical fatigue life prediction model development program at the NASA-Lewis Research Center. The models are still in the development stage, but the data that have been generated possess intrinsic value on their own. The purpose of this paper is to report results generated to date.

Data have been generated to characterize isothermal low-cycle fatigue resistance at temperatures of 316, 704, 760, and 927 C with cyclic failure lives ranging from 10 to more than 20,000. These results follow trends that would be predicted from a knowledge of tensile properties, i.e., as the tensile ductility varies with temperature, so varies the cyclic inelastic straining capacity. Likewise, as the tensile strength decreases, so does the high-cycle fatigue resistance. A few two-minute hold-time cycles at peak compressive strain were included in tests at 760 C. These results were obtained in support of a redesign effort for the Orbital Maneuverable System engine. No detrimental effects on cyclic life were noted despite the added exposure time for creep and oxidation.

Finally, a series of simulated thermal fatigue tests, referred to as bithermal fatigue tests, have been conducted using 316 C as the minimum and 760 C as the maximum temperature. Only out-of-phase bithermal tests have been conducted to date. These test results are intended for use as input to a more general thermomechanical fatigue life prediction model based on the concepts of the total strain version of Strainrange Partitioning.

INTRODUCTION

The wrought cobalt-base superalloy Haynes 188 exhibits excellent high-temperature strength, ductility, and environmental resistance [1]. It has been used for various components in turbine engines in the aeronautics industry. Space related applications for the alloy include the LOX posts (liquid oxygen injection tubes) in the main combustion chamber of the Space Shuttle Main Engine (SSME) [2], potential use in the combustion chamber of the Orbital Maneuvering Engine (OME) [3], and

potential use as a canister material to contain a high-temperature, phase-change salt for thermal storage in a solar receiver system for the Space Station [4]. In support of these projects and the development of advanced life prediction methods [5,6], the Structures Division of the Lewis Research Center has conducted a variety of high-temperature, low- and high-cycle fatigue tests of wrought Haynes 188. The results generated to date are presented for the benefit of other users.

EXPERIMENTAL DETAILS

Haynes 188 Material and Specimen Configuration

The material for this program was purchased from Haynes International of Kokomo, Indiana by the Lewis Research Center in the mid-1970s in support of a now-defunct program. Details of the fabrication and heat treating processes have been lost to history. However, the chemical composition of the 1.6 cm thick rolled plate has since been determined and is listed in table I. In addition, the microstructure has been documented as shown in fig. 1. The material has a hardness of Rockwell 'C' 22 and a grain size of ASTM 7. No tensile test data have been generated on this heat of material. Typical handbook [1] tensile properties are presented in fig. 2 and tabulated in table II. Elastic modulii at the temperatures of interest were interpolated from available data (table II). Fatigue specimens were machined to the hourglass configuration shown in fig. 3. The specimen axis was parallel with the final plate rolling direction. They received no post-machining heat treatment or stress relief.

Our objective in this program was to document the high-temperature, low-cycle fatigue behavior of the Haynes 188 alloy for two major purposes. The first was to provide property data for comparison with other candidate alloys for potential use in and analysis of the OME, SSME LOX posts, and a Space Station thermal storage system. The second reason was to provide validation for a newly developed thermomechanical fatigue life prediction method [5]. Both isothermal and non-isothermal results were obtained. Continuous strain-cycling experiments were performed at 316, 704, 760, and 927 C. Four compressive-strain, two-minute hold time tests were performed at 760 C. Finally, several bithermal fatigue tests were conducted with maximum and minimum temperatures of 760 and 316 C.

Test Equipment

Uniaxial servo-hydraulic testing machines were used to perform all the experiments. The isothermal and bithermal tests were conducted in strain- and load-control (strain limited), respectively. Strains were measured at the minimum cross-section of the hourglass specimen using a diametral extensometer. Specimens were heated to the required temperature in ambient air, using a direct resistance method. Due to the hourglass geometry of the specimen, the maximum temperature occurs at the minimum cross-section. Temperature control was accomplished with a chromel-alumel thermocouple spot-welded to the specimen surface. The

location of the thermocouple was sufficiently remote from the minimum cross-section to prevent premature fatigue crack initiation at the spot weld. Temperature at the minimum cross-section of the hourglass specimen was measured with a disappearing-wire optical pyrometer for temperatures at and above 704 C. For temperatures below 704 C, the temperature at the minimum cross-section of the hourglass specimen was calibrated against the temperature at the remote location (about 0.5 cm from the minimum cross-section) using thermocouples spot welded at both locations on a sacrificial specimen. Once the temperature calibration was known the temperature at the minimum cross-section could be inferred from the temperature of the remote thermocouple.

A commercially available digital computer with appropriate A/D and D/A devices was used to control most of the isothermal and all of the bithermal experiments [7].

Test Procedures

Isothermal Tests:

The required waveforms for conducting HRSC (high-rate, strain-cycling) and CHSC (compressive-hold, strain-cycling) tests, were generated either with a conventional analog function generator or with the computer. The two waveforms are illustrated in fig. 4. The diametral extensometer, supported by eight self-centering springs, was attached at the minimum cross-section of the specimen. The specimen and the extensometer were maintained at the test temperature for at least an hour before each test to achieve thermal equilibrium.

Bithermal Tests:

Schematic hysteresis loops for the HROP (tensile plastic strain at low temperature and compressive plastic strain at high temperature) and CCOP (tensile plastic strain at low temperature and compressive creep strain at high temperature) tests are presented in fig. 5 [8]. Temperature, load rate and total strain limit history were controlled by the computer. The necessary test control software was written in Pascal language. Before conducting a bithermal test, the specimen and extensometer were thermally cycled at zero load between the maximum and minimum temperatures to achieve thermal equilibrium as well as to obtain the thermal expansion strains. The thermal cycle time was 75 seconds for heating and 105 seconds for cooling. The desired mechanical strains were then superimposed on the thermal strains to obtain the total strains required for the control of the test.

Test data were recorded continuously on a strip chart and load versus diametral displacement response was recorded periodically on an X-Y recorder for both isothermal and bithermal experiments. Failure for all tests was defined as a 50% drop in the tensile peak load from a stabilized value. Diametral strains were converted into axial strains using the procedures described in reference [3]. In the case of bithermal

tests, mechanical strains were obtained by subtracting the thermal strains from the measured total strains.

RESULTS AND DISCUSSION

Isothermal Low-Cycle Fatigue Behavior

The isothermal low-cycle fatigue results at 316, 704, 760 & 927 C are summarized together with the stabilized cyclic stress-strain behavior in this section. The isothermal HRSC data at 704 and 760 C were generated by Mike McGaw and Pete Bizon [2], respectively. Robb Duckert assisted in generating the rest of the isothermal data presented in this report. The stress ranges, the elastic, inelastic and total strainranges (determined from the near half-life hysteresis loops), and the cyclic lives are presented in table III. In HRSC tests, Haynes 188 exhibited cyclic hardening at 316, 704 & 760 C. However, at 927 C, no cyclic hardening was observed, indicating that the mechanical work hardening was recovered by thermally activated mechanisms. At these temperatures, hysteresis loops were stable during the interval between approximately 30% and 70% of the cyclic life.

The low-cycle fatigue data in the form of elastic, inelastic and total strainrange versus life curves are plotted in figs. 6 to 9 for the four temperatures investigated in this study. The equations shown in the figures were obtained from a least squares analysis of the data. The plastic strainrange-life lines among these plots indicate that the capacity of Haynes 188 to absorb cyclic inelastic strain decreases as the temperature is increased from 316 C to 704 C, reaches a minimum near 760 C, and increases as the temperature is increased to 927 C. Even though this appears as an erratic behavior, it is consistent with the variation of tensile ductility with temperature of this alloy. Indeed the tensile elongation versus temperature plot (fig. 2), indicates that Haynes 188 has a ductility minimum around 760 C. Since ductility governs the low cycle fatigue resistance of an alloy, the capacity to absorb cyclic inelastic strains also would be expected to reach a minimum around 760 C. There is also a remarkable consistency in the slope of the plastic strainrange-life lines over this temperature range, i.e., -0.695 ± 0.010. The elastic strainrange-life lines of figs. 6 to 9 indicate that, in general, the high cycle fatigue resistance of Haynes 188 decreases as the temperature is increased from 316 C to 927 C. This behavior is to be expected, since the tensile strength of the alloy also decreases with the temperature (fig. 2). Again, the slopes of the elastic strainrange-life lines are reasonably consistent with a value of -0.106 ± 0.025.

The fatigue lives of the four CHSC experiments at 760 C with hold periods of 2 minutes each were not significantly different from the fatigue lives of the HRSC tests at 760 C (fig. 10). This indicates that compressive strain holds are not detrimental to the fatigue life in this regime. Mean stresses were negligible in these tests. However, experi-

ments with long compressive hold times would be necessary to conclusively establish the effect of compressive hold time on cyclic life.

Bithermal Low-Cycle Fatigue Behavior

The out-of-phase bithermal stress-strain response and fatigue results between 316 and 760 C are summarized in this section. Robb Duckert assisted in the generation of some of the bithermal fatigue data presented in this report. The stress ranges, the elastic, plastic & total strainranges, (determined from the near half-life hysteresis loops) and the cyclic lives for the experiments are presented in table IV. In general, the out-of-phase bithermal experiments exhibited more hardening than isothermal experiments. In the case of HROP experiments, the tensile half-loop (lower temperature) exhibited more severe hardening than the compressive half-loop (higher temperature). For CCOP experiments, since creep was induced in compression at the higher temperature, all of the hardening was observed in the tensile half-loop at the lower temperature. Unlike the isothermal hysteresis loops, the bithermal hysteresis loops hardened for a longer proportion of the life of the specimen, with smaller stabilized periods.

The bithermal data are plotted along with the isothermal plastic lines for the maximum and minimum temperatures of the bithermal loop in fig. 11. It is interesting to note that the bithermal data (both HROP and CCOP) are very close to the plastic life line at 760 C. This is contradictory to the generally held belief [9] that the tensile portion of a cycle governs cyclic life, i.e., the bithermal results would have been expected to lie closer to the plastic strainrange-life line at 316 C. More critical experiments will be necessary to explain this behavior. Metallographic investigations are currently in progress to understand the micromechanisms involved in bithermal fatigue, and for comparison with the isothermal behavior.

SUMMARY AND CONCLUSIONS

The high-temperature, low-cycle, isothermal and bithermal fatigue behavior of the wrought cobalt-base superalloy, Haynes 188 has been investigated and documented.

Results are presented in terms of the cyclic stress-strain response and elastic, inelastic and total strain range versus cycles to failure curves. Isothermal continuous strain cycling tests at frequencies of between 0.2 and 29 Hz were performed at four isothermal temperatures ranging from 316 to 927 C. Compressive strain hold time tests were conducted at 760 C.

Out-of-phase bithermal fatigue tests were performed between the temperatures of 316 and 760 C.

Cyclic hardening was observed in isothermal HRSC experiments conducted at 316, 704 & 760 C, but not at 927 C. During out-of-phase bithermal

fatigue experiments Haynes 188 exhibited more cyclic strain hardening than during isothermal fatigue.

Isothermal continuous strain cycling fatigue results are consistent with what one would expect based upon handbook tensile data, i.e., the plastic strainrange versus life curve drops as tensile ductility drops with increasing temperature until a minimum is observed, then the ductility and the low-cycle fatigue curve begin to increase again. The elastic strainrange versus life curve drops continuously as temperature increases and ultimate tensile strength decreases. There is no observed decrease in high-temperature fatigue resistance due to a 2 minute compressive hold time compared to the continuous strain cycling results at 760 C.

Finally, the bithermal fatigue results unexpectedly tended to follow the life trends corresponding to the temperature and straining conditions of the compressive half of the cycle, i.e., they followed the data trends for the 760 C isothermal results rather than the 316 C isothermal results.

The results reported herein are being used in support of hardware design problems as well as for the validation of a high-temperature life prediction method for thermomechanical fatigue that is based on the total strain version of Strainrange Partitioning.

REFERENCES

1. Anon.: High Temperature High Strength Nickel Base Alloys, International Nickel Company, Inc., 1977, pp. 21-24.

2. Bizon, P. T.; Thoma, D. J.; and Halford, G. R.: Interaction of High Cycle and Low Cycle Fatigue of Haynes 188 at 1400 F, Structural Integrity and Durability of Reusable Space Propulsion Systems, NASA CP-2381, 1985, pp. 129-138.

3. Halford, G. R.; Johnson, L. R.; and Brown, J. A.: High-Temperature LCF of Ni-201 and 304L SS. Advanced Earth-to-Orbit Propulsion Technology 1986, Volume II, NASA CP 2437, 1986, pp. 172-204. (Limited Distribution Document, General Release Date: October 1988).

4. Ellis, J. R.; Bartolotta, P. A.; and Mladsi, S. W.: Preliminary Study of Creep Thresholds and Thermomechanical Response in Haynes 188 at Temperatures in the Range 649 to 871 C. Turbine Engine Hot Section Technology 1987, NASA CP 2493, 1987, pp. 317-334 (Limited Distribution Document, General Release Date: October 1989).

5. Saltsman, J. F.; and Halford, G. R.: Life Prediction of Thermomechanical Fatigue Using Total Strain Version of Strainrange Partitioning (SRP)---A Proposal. NASA TP-2779, February 1988.

6. Halford, G. R.; Saltsman, J. F.; Verrilli, M. J.; Kalluri, S.;

Ritzert, F. J.; and Duckert, R. E.: Thermal Fatigue Life Prediction -- A New Approach Based on Bithermal Fatigue, Strainrange Partitioning and Cyclic Constitutive Models. Submitted for presentation at the Symposium on Constitutive Equations and Life Prediction Models for High Temperature Applications, University of California, Berkeley, June 20-22, 1988.

7. McGaw, M. A. and Bartolotta, P. A.: A High Temperature Fatigue and Structures Testing Facility. Proceedings, 4th Annual Hostile Environments and High Temperature Measurements Conference, Society for Experimental Mechanics, Bethel, CT, 1987, pp. 12-29. (See also NASA TM-100151, 1987).

8. Halford, G. R.; McGaw, M. A.; Bill, R. C.; and Fanti, P. D.: Bithermal Fatigue, A Link Between Isothermal and Thermomechanical Fatigue. Low Cycle Fatigue, ASTM STP 942, H. D. Solomon, G. R. Halford, L. R. Kaisand, and B. N. Leis, Eds., American Society for Testing and Materials, Philadelphia, 1988, pp. 625-637.

9. Halford, G. R.; Saltsman, J. F; and Hirschberg, M. H.: Ductility-Normalized Strainrange Partitioning Life Relations for Creep-Fatigue Life Predictions. Environmental Degradation of Engineering Materials, M.R. Louthan and R.P. McNitt, Eds., Virginia Tech Printing Dept., Blacksburg, VA, 1977, pp. 599-612.

TABLE I
HAYNES 188 : CHEMICAL COMPOSITION

Element	Weight %
Nickel	21.00
Chromium	22.30
Tungsten	17.80
Manganese	3.60
Silicon	0.40
Carbon	0.10
Nitrogen	0.06
Iron	1.6 ppm
Lanthanum	< 0.3 ppm
Cobalt	Balance

TABLE II
HAYNES 188 : TENSILE PROPERTIES

Temp (C)	E (GPa)	Ultimate (MPa)	Yld, 0.2% (MPa)	Elongation, %
21	216	960	485	56
93	214*	-	-	
204	209	-	-	
316	204*	-	-	
427	199	-	-	
538	192*	740	305	70
649	185	710	305	61
704	181*	-	-	
760	175*	635	290	43
871	166	420	260	73
927	160*	-	-	
982	155*	255	165	72
1093	142	130	83	47

* Interpolated values

TABLE III
HAYNES 188 : ISOTHERMAL DATA

SPECIMEN NUMBER	TEST TYPE	TEMP (C)	FREQ (Hz)	STSRANGE (MPa)	ELASTIC STNRANGE	PLASTIC STNRANGE	TOTAL STNRANGE	CYCLIC LIFE
HA-92	HRSC	316	0.2	1276	0.00625	0.02546	0.03171	995
HA-104	HRSC	316	0.2	1118	0.00548	0.01051	0.01599	4959
HA-87	HRSC	316	0.2	967	0.00474	0.00349	0.00823	17678
HA-4	HRSC	704	0.2	1425	0.00789	0.01577	0.02366	281
HA-3	HRSC	704	0.5	1248	0.00691	0.00940	0.01631	524
HA-27	HRSC	704	0.5	1215	0.00673	0.00867	0.01540	954
HA-25	HRSC	704	0.5	1208	0.00669	0.00828	0.01497	652
HA-28	HRSC	704	0.5	1187	0.00657	0.00838	0.01495	885
HA-2	HRSC	704	0.5	1134	0.00628	0.00527	0.01155	1477
HA-43	HRSC	704	0.5	889	0.00492	0.00298	0.00790	3797
HA-5	HRSC	704	0.5	780	0.00432	0.00185	0.00617	15705
HA-6	HRSC	704	0.5	818	0.00453	0.00106	0.00559	22125
HA-13	HRSC	704	0.5	836	0.00463	0.00042	0.00505	51438
HA-18	HRSC	704	0.5	759	0.00420	0.00064	0.00484	21399
HA-47	HRSC	760	0.4	1672	0.00955	0.08904	0.09859	13
HA-32	HRSC	760	0.4	1121	0.00640	0.00900	0.01540	302
HA-40	HRSC	760	0.4	1037	0.00592	0.00678	0.01270	400
HA-35	HRSC	760	0.4	1086	0.00620	0.00625	0.01245	445
HA-31	HRSC	760	0.4	1084	0.00619	0.00407	0.01026	1370
HA-36	HRSC	760	0.4	1180	0.00674	0.00255	0.00929	709
HA-45	HRSC	760	0.4	877	0.00501	0.00307	0.00808	2142
HA-64	HRSC	760	0.4	1026	0.00586	0.00210	0.00796	1977
HA-61	HRSC	760	29.0	835	0.00477	0.00145	0.00622	4500
HA-37	HRSC	760	0.4	819	0.00468	0.00105	0.00573	4918
HA-78	HRSC	760	29.0	807	0.00461	0.00100	0.00561	7900
HA-54	HRSC	760	29.0	742	0.00424	0.00111	0.00535	11300
HA-74	CHSC	760	0.2	1237	0.00593	0.01693	0.02286	233
HA-80	CHSC	760	0.2	1278	0.00597	0.01618	0.02215	219
HA-52	CHSC	760	0.2	1068	0.00506	0.00624	0.01130	803
HA-73	CHSC	760	0.2	1018	0.00499	0.00604	0.01103	822
HA-100	HRSC	927	0.2	666	0.00416	0.01798	0.02214	372
HA-101	HRSC	927	0.2	645	0.00403	0.01786	0.02189	295
HA-93	HRSC	927	0.2	568	0.00355	0.00783	0.01138	1985
HA-102	HRSC	927	0.2	605	0.00378	0.00738	0.01116	921
HA-103	HRSC	927	0.2	488	0.00305	0.00158	0.00463	12568
HA-105	HRSC	927	0.2	496	0.00310	0.00144	0.00454	10885

CHSC tests have 2 minute compressive hold time

TABLE IV
HAYNES 188 : OUT-OF-PHASE BITHERMAL DATA
TEMPERATURE RANGE : 316 - 760 C

SPECIMEN NUMBER	TEST TYPE	MAXSTRSS (MPa)	MINSTRSS (MPa)	ELASTIC STNRANGE	PLASTIC STNRANGE	TOTAL STNRANGE	Tf ** (Hrs)	CYCLIC LIFE
HA-94 *	HROP	823	-776	0.00846	0.03274	0.04120	3.5	58
H-113	HROP	823	-796	0.00858	0.01668	0.02526	12.0	213
HA-85	HROP	806	-734	0.00814	0.01296	0.02110	18.5	304
HA-88	HROP	737	-660	0.00738	0.00687	0.01425	47.4	682
H-114	HROP	692	-643	0.00705	0.00559	0.01265	56.7	955
H-112	HROP	620	-570	0.00629	0.00339	0.00968	163.2	2799
HA-99	CCOP	815	-333	0.00589	0.02659	0.03248	62.1	52
H-101	CCOP	736	-332	0.00550	0.01054	0.01604	266.0	215
HA-86	CCOP	664	-299	0.00496	0.00564	0.01060	133.9	647

* Some creep strain occured due to the large compressive stresses at 760 C
** Includes thermal cycling time under no load and mechanical loading time

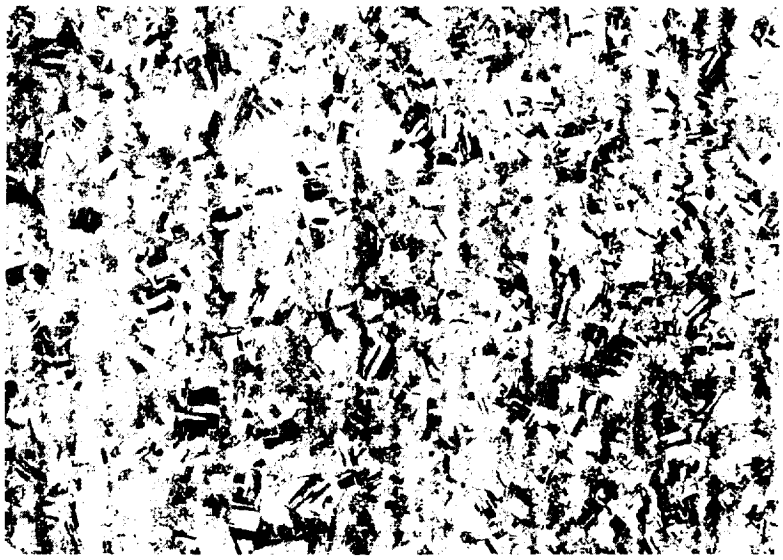

100 X

Fig. 1 Microstructure of Haynes 188.

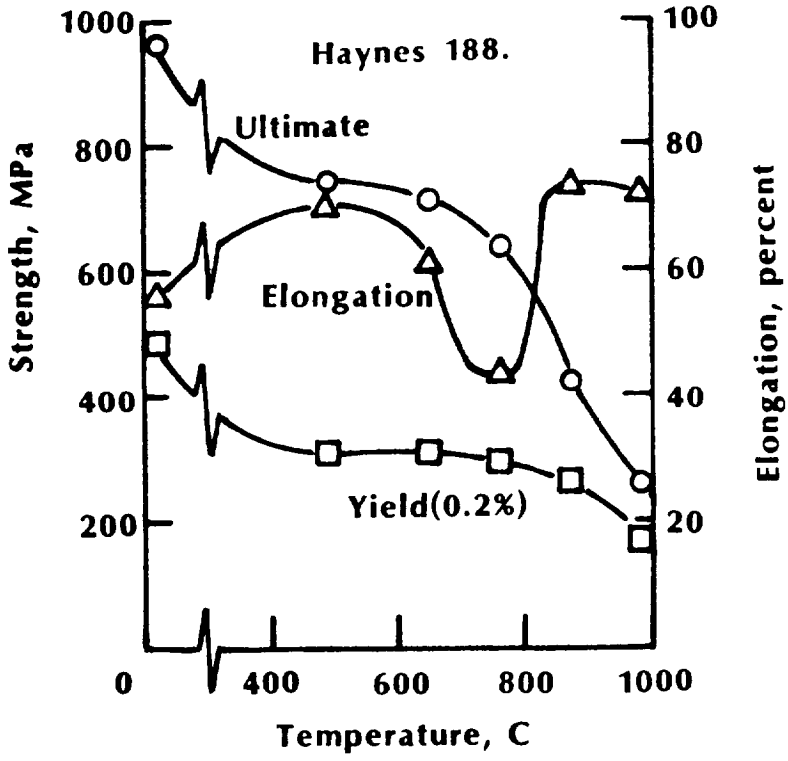

Fig. 2 Temperature Dependence of Tensile Properties

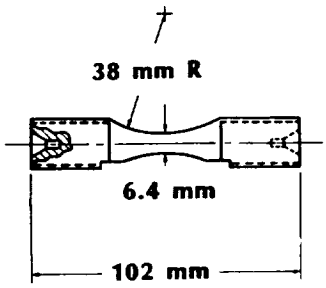

Fig. 3 Hourglass Specimen Geometry.

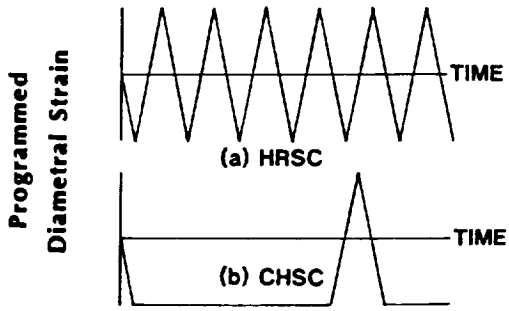

Fig. 4 Isothermal Strain vs. Time Waveforms

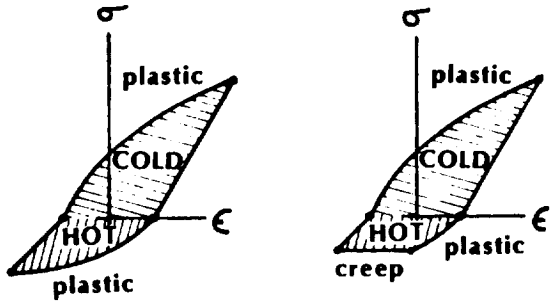

(a) Out of Phase PP (b) Out of Phase PC

Fig. 5 Schematic Representation of Bithermal Hysteresis Loops

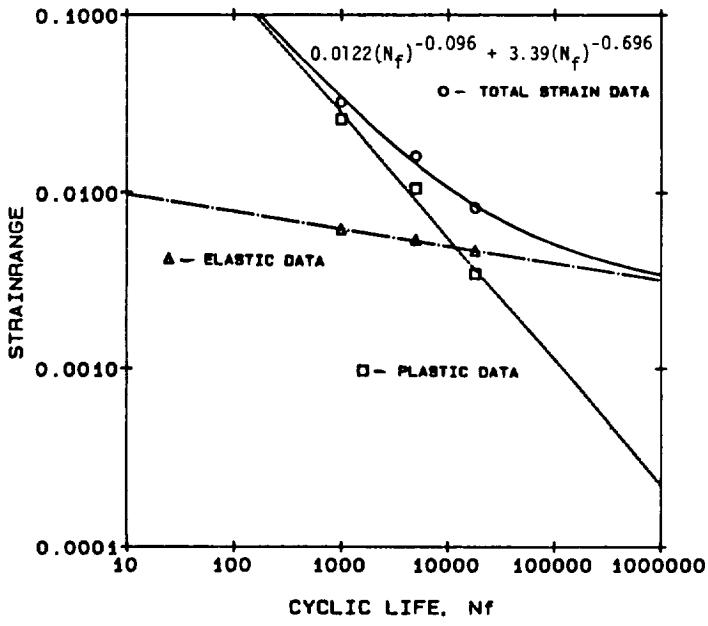

Fig. 6 Isothermal LCF Behavior of Haynes 188 at 316 C.

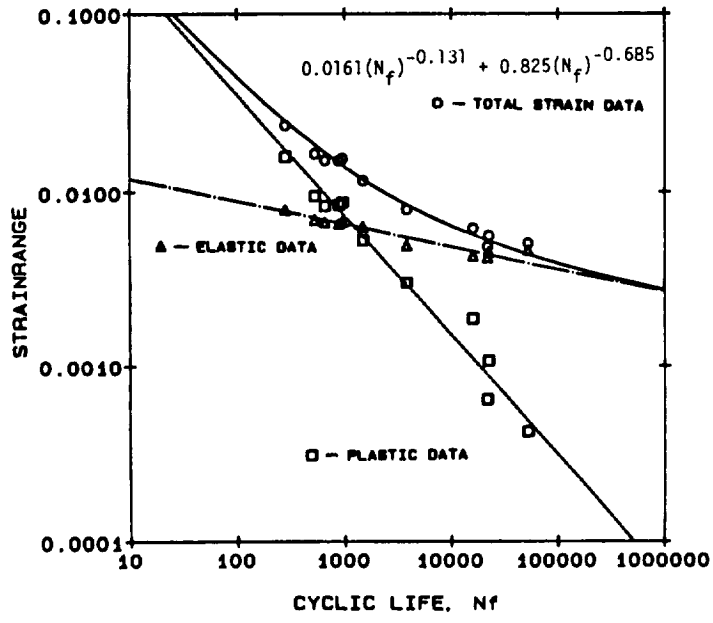

Fig. 7 Isothermal LCF Behavior of Haynes 188 at 704 C.

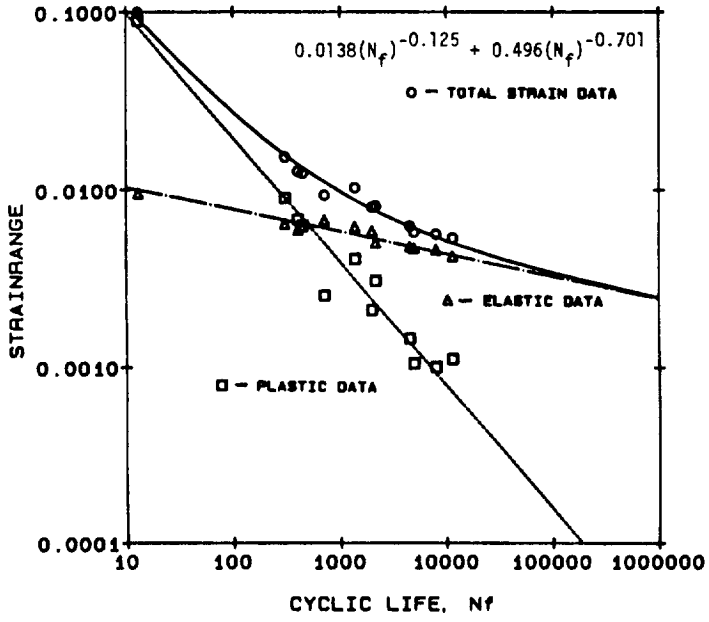

Fig. 8 Isothermal LCF Behavior of Haynes 188 at 760 C.

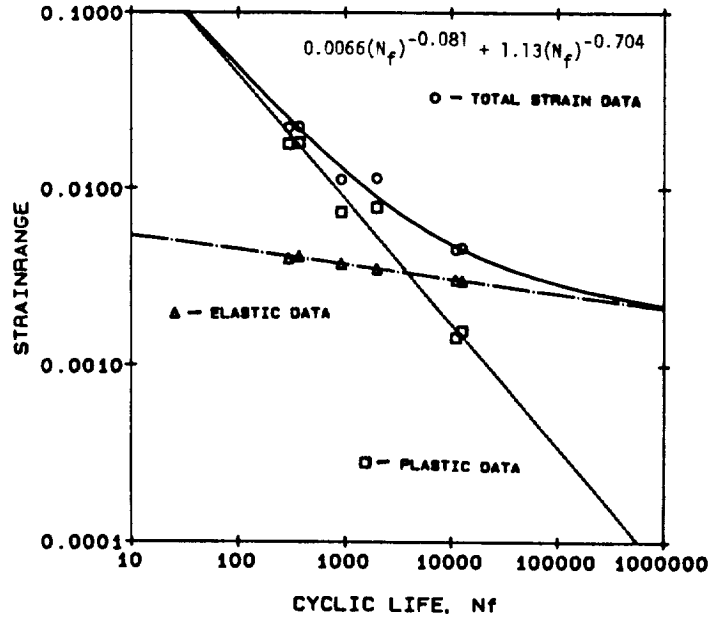

Fig. 9 Isothermal LCF Behavior of Haynes 188 at 927 C.

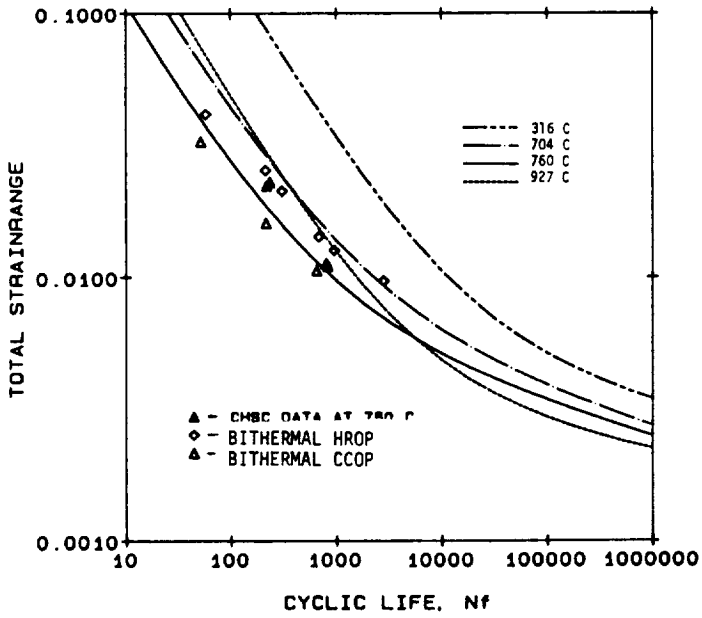

Fig. 10 Summary of LCF Results for Haynes 188.

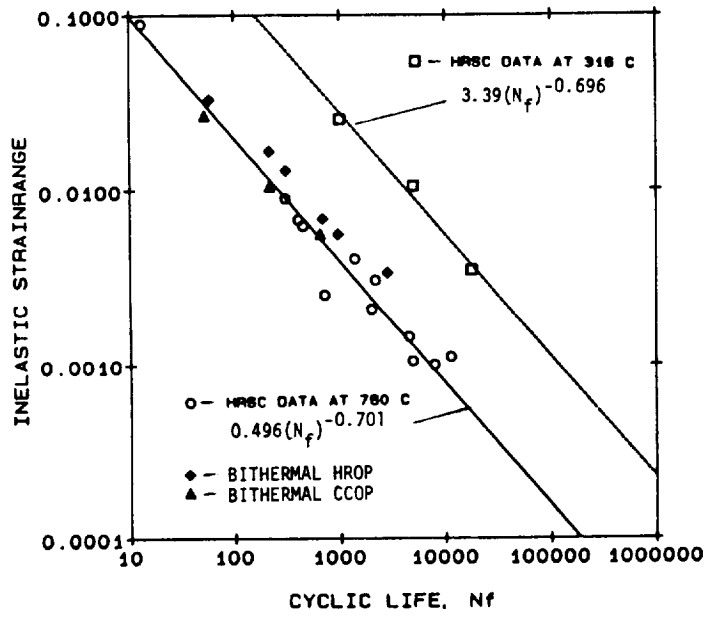

Fig. 11 Inelastic Strain Range vs. Life Relations for Haynes 188.